Crossover SAFT Equation of State: Application for Normal Alkanes

S. B. Kiselev* and J. F. Ely

Chemical Engineering and Petroleum Refining Department, Colorado School of Mines, Golden, Colorado 80401-1887

In this paper we develop a crossover modification of the statistical associating fluid theory (SAFT) equation of state for macromolecular chain fluids which incorporates the scaling laws asymptotically close to the critical point and is transformed into the original classical SAFT equation of state far away from the critical point. A comparison is made with experimental data for pure methane, ethane, *n*-hexane, *n*-decane, and *n*-eicosane in the one- and two-phase regions. We also present comparisons with experimental single-phase data for *n*-triacontane and *n*-tetracontane. We show that, over a wide range of states, the crossover SAFT model yields a much better representation of the thermodynamic properties of pure fluids than the original SAFT equation of state. The crossover SAFT equation of state reproduces the saturated pressure data in the entire temperature range from the triple point to the critical temperature with an average absolute deviation (AAD) of about 3.8%, the saturated liquid densities with an AAD of about 1.5%, and the saturated vapor densities with an AAD of about 3.4%. In the one-phase region, the crossover SAFT equation represents the experimental values of pressure in the critical region with an AAD of about 2.9% in the region bounded by $0.05\rho_c \le \rho \le 2.5\rho_c$ and $T_c \le T \le 2T_c$, and the liquid density data with an AAD of about 3% at the pressures up to $P = 2000$ bar. For the *n*-alkanes C_mH_{2m+2} with the molecular weight $M_w > 142$ ($m > 10$), the crossover SAFT model contains no adjustable parameters and can be used for the pure prediction of the fluid thermodynamic surface.

1. Introduction

The development of a universal model for the prediction of the thermodynamic properties of macromolecular chain fluids and their mixtures has always been one of the most difficult tasks in the theory of fluids. The strong cooperative interactions between the molecules even in simple liquids do not allow a general calculation of their thermodynamic quantities over a wide range of states. In the case of polymeric materials, increasing the size of the molecule and the presence of association add extra complications, which have never been accurately included in modern theories.

In recent years, concentrated efforts have been made to develop molecularly based equations of state (EOS) for polymeric fluids. These models range from simple cubic equations of state, which are widely used in the engineering calculations, to more sophisticated free energy models based on statistical mechanics, such as the perturbed hard-sphere chain theory (PHSCT)[1−8] or the statistical associating fluid theory (SAFT).[9−18] Simple cubic EOS, such as ones developed by Redlich and Kwong,[19] Soave,[20] and Peng and Robinson,[21] yield reasonable representations of the thermodynamic properties of fluids and fluid mixtures with low molecular weight components, but they give the large errors for long-chain molecular fluids and mixtures of components which differ greatly in size or polarity.[22−27] For these systems, the PHSCT and SAFT models give better results than the simple cubic EOS.[28−32]

In general, the chain fluid models work reasonably well, especially at high-to-moderate polymer concentrations. A major difference between them is in their abilities to predict PVT properties of polymer and polymer blends over a wide range of temperatures and densities in the supercritical region, and particularly the vapor−liquid (VLE) and liquid−liquid (LLE) equilibria. However, in situations where the system possesses long-range correlations, such as near a critical point or at low polymer concentrations, these models fail to yield an accurate description of the thermodynamic behavior.

At the same time, the thermodynamic behavior of simple fluids in the critical region has been studied in great detail. The critical point of a one-component fluid is the simplest case of a second-order phase transition and is a typical example of cooperative behavior in a fluid system. A characteristic feature of fluids in the vicinity of the critical point is the presence of the long-range fluctuations in the density, which involve a huge number of molecules. Therefore, in the critical region the details of the intermolecular interaction become irrelevant to the thermodynamic behavior of the system, which is completely determined by the interaction of the fluctuations, and as a consequence, the thermodynamic surface of fluids exhibit a singularity at the critical point. The asymptotic singular critical behavior of the thermodynamic properties can be described in terms of scaling laws with universal critical exponents and universal scaling functions.[33,34] The thermodynamics of a system in the extended critical region can be described in terms of scaling laws with universal crossover functions. These crossover functions reproduce the asymptotic scaling laws in the nearest vicinity of the critical point and transform the Helmholtz free energy of the system into the classical-analytical form far away from the critical point.

* To whom correspondence should be addressed. Phone: (303) 273-3190. Fax: (303) 273-3730. E-mail: skiselev@mines.edu.

10.1021/ie990387i CCC: $18.00
Published on Web 10/26/1999

Theoretical crossover equations of state for pure fluids and binary mixtures which incorporate the scaling laws asymptotically close to the critical point and are transformed into the regular classical expansion far away from the critical point have been developed by Sengers and co-workers[35,36] and by Kiselev et al.[37−41] Although these crossover equations of state give a very accurate representation of the thermodynamic properties of fluids and fluid mixtures in a wide region around the critical point, in the limit of zero density they do not reproduce the ideal gas equation of state and, therefore, they cannot be extrapolated to low densities.

A general procedure for transforming any classical equation of state into a crossover EOS which incorporates the scaling laws asymptotically close to the critical point and is transformed into the original classical EOS far from the critical point was proposed by Kiselev.[42] This procedure has a theoretical foundation in the renormalization-group theory and has been successfully applied to the cubic Patel−Teja (PT) EOS.[43] The incorporation of the effects of the critical fluctuations into the cubic EOS gives a major improvement of the representation of the thermodynamic surface of fluids in and beyond the critical region.[42,44,45] As was shown by Kiselev and co-workers,[42,44] incorporation of the universal crossover functions into the original PT EOS not only yields a better description of the *PVT* and VLE properties of pure fluids and binary mixtures in the critical region but also improves the representation of the thermodynamic surface of dense fluids in general.

It is the aim of this paper to develop, on the basis of Kiselev's approach,[42] a crossover SAFT equation of state for pure fluids which incorporates the scaling laws asymptotically close to the critical point and is transformed into the original SAFT equation of state far away from the critical point. We proceed as follows. In section 2 we describe the original SAFT model. In section 3 we formulate the crossover expression for the Helmholtz free energy for the SAFT EOS. Comparisons with experimental data for pure *n*-alkanes are discussed in section 4. Our results are summarized in section 5.

2. Original SAFT Equation

In the present work we apply the crossover theory to the SAFT equation of state developed by Huang and Radosz.[10] The original SAFT EOS is given in terms of the residual Helmholtz free energy per mole:

$$a(T, V, N) = a^{\mathrm{res}}(T, V, N) + a^{\mathrm{ideal}}(T, V, N) \quad (1)$$

where $a(T, V, N)$ is the total Helmholtz free energy, $a^{\mathrm{res}}(T, V, N)$ is the residual Helmholtz free energy, and $a^{\mathrm{ideal}}(T, V, N) = -RT \ln(V/N) + a_0(T)$ is the ideal gas Helmholtz free energy per mole at the same temperature T and the molar volume $v = V/N$. The residual Helmholtz free energy a^{res} is represented in the SAFT model as a sum of three terms corresponding to the contributions from three different intermolecular interactions:

$$a^{\mathrm{res}} = a^{\mathrm{seg}} + a^{\mathrm{chain}} + a^{\mathrm{assoc}} \quad (2)$$

The first term on the right side of eq 2 represents segment−segment interaction,

$$a^{\mathrm{seg}} = m a_0^{\mathrm{seg}} \quad (3)$$

where a^{seg} is the Helmholtz free energy of a nonassociated spherical segment and m is the number of segments. In the SAFT EOS a_0^{seg} is composed of two parts,[10]

$$a_0^{\mathrm{seg}} = a_0^{\mathrm{hs}} + a_0^{\mathrm{disp}} \quad (4)$$

where for the hard-sphere contribution a_0^{hs} the Carnahan−Starling equation is used,[46]

$$a_0^{\mathrm{hs}} = RT\frac{4\eta - 3\eta^2}{(1-\eta)^2} \quad (5)$$

while for the dispersion term a_0^{disp} the power series proposed by Alder et al.[47] for square-well fluids was adopted:

$$a_0^{\mathrm{disp}} = RT\sum_i\sum_j D_{ij}\left(\frac{u}{kT}\right)^i\left(\frac{\eta}{\eta_0}\right)^j \quad (6)$$

In eqs 5 and 6, R is the universal gas constant, k is the Boltzmann constant, and the reduced density is

$$\eta = \eta_0 m v^0/v \quad (7)$$

where $\eta_0 = 0.74048$, v^0 is the segment molar volume in a close-packed arrangement, u is the well depth, and D_{ij} are universal constants which have been fitted to the experimental data for argon by Chen and Kreglewski.[48] Following Chen and Kreglewski,[48] the parameters v^0 and u were represented in the form

$$v^0 = v^{00}\left[1 - C\exp\left(\frac{-3u^0}{kT}\right)\right]^3 \quad (8)$$

$$u = u^0\left(1 + \frac{e}{kT}\right) \quad (9)$$

where $C = 0.12$, $e/k = 10$, and v^{00} and u^0 are the system-dependent parameters.

The second term on the right side of eq 2 is the chain term, which is the same as the one described by Chapman et al.,[9]

$$a^{\mathrm{chain}} = RT(1-m)\ln g^{\mathrm{hs}}(\eta) \quad (10)$$

where for the hard-sphere radial distribution function the Carnahan−Starling approximation[46] is used:

$$g^{\mathrm{hs}}(\eta) = \frac{2-\eta}{2(1-\eta)^3} \quad (11)$$

The Helmholtz free energy change due to association, the third term in eq 2, is given by

$$a^{\mathrm{assoc}} = RT\left[\sum_{\mathrm{A}}\left(\ln X^{\mathrm{A}} - \frac{X^{\mathrm{A}}}{2}\right) + \frac{1}{2}M\right] \quad (12)$$

where M is the number of association sites on each molecule, X^{A} is the mole fraction of molecules not bonded at site A, and $\sum_{\mathrm{A}}$ represents a sum over all associating

sites on the molecule. The mole fraction of nonbonded molecules is represented in the SAFT EOS as

$$X^{A} = (1 + N_{A}\sum_{B} X^{B}\Delta^{AB})^{-1} \quad (13)$$

where the summation over all sites A, B, C, ... is provided, N_A is Avogadro's number, and

$$\Delta^{AB} = \kappa^{AB}\frac{6\eta_0 v^{00}}{\pi N_A}[\exp(\epsilon^{AB}/kT) - 1]g^{hs}(\eta) \quad (14)$$

The critical parameters T_{0c}, v_{0c}, and P_{0c} corresponding to the classical SAFT equation of state can be found from the conditions

$$P_{0c} = -\left(\frac{\partial a}{\partial v}\right)_{T_{0c}}, \quad \left(\frac{\partial^2 a}{\partial v^2}\right)_{T_{0c}} = 0, \quad \left(\frac{\partial^3 a}{\partial v^3}\right)_{T_{0c}} = 0 \quad (15)$$

which for the SAFT EOS can be solved only numerically. In general, the critical parameters in the SAFT EOS (T_{0c}, v_{0c}, P_{0c}) are the complicated functions of the parameters m, v^{00}, ϵ^{AB}, and κ^{AB}.

3. Crossover SAFT Model

A simple method for incorporating scaling laws into an analytical equation of state has been developed by Kiselev.[42] The crossover function in this method does not depend on the particular type of classical EOS to be renormalized, and it can be applied to any analytical equation of state.

To apply this method to the SAFT equation of state, one first rewrites the classical expression for the Helmholtz free energy in the dimensionless form

$$\bar{A}(T, v) = \frac{a(T, V, N)}{RT} = \Delta\bar{A}(\Delta T, \Delta v) - \Delta v\bar{P}_0(T) + \bar{A}_0^{r}(T) + \bar{A}_0(T) \quad (16)$$

where $\bar{P}_0(T) = P(T, v_{0c})v_{0c}/RT$ and $\bar{A}_0^{r}(T) = a^{res}(T, v = v_{0c})/RT$ are the dimensionless pressure and the dimensionless residual part of the Helmholtz free energy along the critical isochore $v = v_{0c}$, and $\bar{A}_0(T) = a_0(T)/RT$ is the dimensionless temperature-dependent part of the ideal gas Helmholtz free energy. The critical part of the Helmholtz free energy is written in the form

$$\Delta\bar{A}(\Delta\bar{T}, \Delta v) = \bar{A}^{r}(\Delta T, \Delta v) - \bar{A}^{r}(\Delta T, 0) - \ln(\Delta v + 1) + \Delta v\bar{P}_0(\Delta T) \quad (17)$$

where the dimensionless residual part of the Helmholtz free energy

$$\bar{A}^{r}(\Delta T, \Delta v) = a^{res}(\Delta T, \Delta v)/RT \quad (18)$$

and the dimensionless pressure at the critical isochore

$$\bar{P}_0(\Delta T) = 1 - \left(\frac{\partial\bar{A}^{r}}{\partial\Delta v}\right)_{\Delta T(\Delta v=0)} \quad (19)$$

are expressed as functions of the dimensionless deviation of the temperature from the classical critical temperature $\Delta T = T/T_{0c} - 1$ and the classical order parameter $\Delta v = v/v_{0c} - 1$.

Secondly, one must replace the classical dimensionless temperature ΔT and volume Δv in the critical part of the Helmholtz free energy as given by eq 17 with the renormalized values

$$\bar{\tau} = \tau Y^{-\alpha/2\Delta_1} + (1 + \tau)\Delta\tau_c Y^{2(2-\alpha)/3\Delta_1} \quad (20)$$

$$\Delta\bar{\eta} = \Delta\eta Y^{(\gamma-2\beta)/4\Delta_1} + (1 + \Delta\eta)\Delta\eta_c Y^{(2-\alpha)/2\Delta_1} \quad (21)$$

so that $\Delta T \rightarrow \bar{\tau}$ and $\Delta v \rightarrow \Delta\bar{\eta}$ in eq 17; this transformation is not applied to $\bar{P}_0(T)$ and $\bar{A}_0^{r}(T)$ in eq 16. In eqs 20 and 21, $\tau = T/T_c - 1$ is the dimensionless deviation of the temperature from the real critical temperature T_c and $\Delta\eta = v/v_c - 1$ is the real order parameter. The factors $\Delta\tau_c = \Delta T_c/T_{0c} = (T_c - T_{0c})/T_{0c}$ and $\Delta\eta_c = \Delta v_c/v_{0c} = (v_c - v_{0c})/v_{0c}$ are the dimensionless shifts of the real critical temperature T_c and the real critical volume v_c from the classical values T_{0c} and v_{0c} determined from eq 15.

The crossover function Y in eqs 20 and 21 can be written in the parametric form[44]

$$Y(q) = \left(\frac{q}{1 + q}\right)^{2\Delta_1} \quad (22)$$

which corresponds to the theoretical crossover function obtained recently by Belyakov et al.[49] in the first order of an ϵ expansion. The parametric variable q, which has a meaning of a renormalized measure of the distance from the critical point, can be found from the solution of the equation

$$q^2 = \frac{\tau}{Gi} + b^2\left(\frac{\Delta\eta}{Gi^{\beta}}\right)^2[1 + d_1\tau(1 - 2\tau) + v_1\Delta\eta^2\exp(-\delta_1\Delta\eta)]^2\left(\frac{q}{1 + q}\right)^{2(1-2\beta)} \quad (23)$$

where $b^2 = 1.359$ is a universal linear-model parameter and Gi is the Ginzburg number for the fluid of interest.[42,44] The first term $\propto d_1\tau$ in the square brackets on the right-hand side of eq 23 corresponds to a projection of the rectilinear diameter of the coexistence curve in the temperature−density variables $\rho_d = (\rho_G + \rho_L)/2 = \rho_c(1 + d_1\tau)$ on the temperature−volume plane $v_d = 1/\rho_d \cong v_c(1 + d_1\tau - 2d_1\tau^2)$.[42] The second term $\propto v_1 \times \exp(-\delta_1\Delta\eta)$ in the square brackets effectively takes into account the asymmetry of the crossover function $Y(q)$ with respect to a transformation $\Delta\eta \rightarrow -\Delta\eta$ which provides the physically obvious condition $Y(q) \rightarrow 1$ at $v \ll v_c$.[44] In our previous discussion of the crossover model,[44] we have shown that the parameter δ_1 is not sensitive to the choice of fluid, and this parameter can be considered constant $\delta_1 = 8.5$.

To complete the transformation of the classical Helmholtz free energy into the crossover form, one needs next to add to eq 16 the kernel term

$$K(\tau^2) = \frac{1}{2}a_{20}\tau^2(Y^{-\alpha/\Delta_1} - 1) + \frac{1}{2}a_{21}\tau^2(Y^{-(\alpha-\Delta_1)/\Delta_1} - 1) \quad (24)$$

where the first term corresponds to the asymptotic limit and the second term to the first Wegner correction for the isochoric specific heat.[50] In eqs 20−24, $\gamma = 1.24$, $\beta = 0.325$, $\alpha = 2 - \gamma - 2\beta = 0.110$, and $\Delta_1 = 0.51$ are the best estimates of the nonclassical critical exponents.[33,34]

Finally, from eq 16, the crossover expression for the Helmholtz free energy can be written in the form

$$\bar{A}(T, v) = \Delta\bar{A}(\bar{\tau}, \Delta\bar{\eta}) - \Delta v\bar{P}_0(T) + \bar{A}_0^{\mathrm{r}}(T) + \bar{A}_0(T) - K(\tau^2) \quad (25)$$

where the critical part $\Delta\bar{A}$ (see eq 17) is given by

$$\Delta\bar{A}(\bar{\tau}, \Delta\bar{\eta}) = \bar{A}^{\mathrm{r}}(\bar{\tau}, \Delta\bar{\eta}) - \bar{A}^{\mathrm{r}}(\bar{\tau}, 0) - \ln(\Delta\bar{\eta} + 1) + \Delta\bar{\eta}\bar{P}_0(\bar{\tau}) \quad (26)$$

The crossover SAFT equation of state can be obtained from the crossover expression (25) by differentiation with respect to volume

$$P(T, v) = -\left(\frac{\partial A}{\partial v}\right)_T = \frac{RT}{v_{0c}}\left[-\frac{v_{0c}}{v_c}\left(\frac{\partial\Delta\bar{A}}{\partial\Delta\eta}\right)_T + \bar{P}_0(T) + \frac{v_{0c}}{v_c}\left(\frac{\partial K}{\partial\Delta\eta}\right)_T\right] \quad (27)$$

The exact expressions for $\bar{A}^{\mathrm{r}}(\bar{\tau}, \Delta\bar{\eta})$, $\bar{A}^{\mathrm{r}}(\bar{\tau}, 0)$, and $\bar{P}_0(\bar{\tau})$ as functions of the renormalized temperature $\bar{\tau}$ and the order parameter $\Delta\bar{\eta}$ for the SAFT EOS are given in the Appendix.

Equations 20−26 completely determine the crossover Helmholtz free energy for the SAFT equation of state. Asymptotically close to the critical point $q \ll 1$ ($|\tau| \ll Gi$ on the critical isochore), the crossover function $Y(q) \propto q^{2\Delta_1}$, the renormalized temperature $\bar{\tau} \propto \tau q^{-\alpha}$ ($\bar{\tau} \propto \tau^{(2-\alpha)/2}$ on the critical isochore), the renormalized volume $\Delta\bar{\eta} \propto \Delta\eta q^{(\gamma-2\beta)/2}$ ($\Delta\bar{\eta} \propto \Delta\eta^{(\gamma-2\beta)/4\beta}$ on the critical isotherm), and the critical part of the free energy $\Delta\bar{A}(\bar{\tau}, \Delta\bar{\eta})$ is a singular nonanalytic function of τ and $\Delta\eta$. In this region, the vapor−liquid coexistence curve $\Delta\rho_s$, the singular part of the isochoric specific heat $\Delta\bar{C}_v = T_c^2\rho_c\Delta C_v/TP_c$, and the reduced susceptibility $\bar{\chi}_T = P_c(\partial\rho/\partial P)_T/\rho_c$ along the critical isochore satisfy the following asymptotic laws:

$$\Delta\rho_s = \pm B_0(-\tau)^\beta, \quad \Delta\bar{C}_v = \alpha^{-1}A_0^+\tau^{-\alpha}, \quad \bar{\chi}_T = \Gamma_0^+\tau^{-\gamma} \quad (28)$$

According to the fluctuation theory of critical phenomena the critical amplitudes in eq 28 are the system-dependent parameters, but only two of them are independent such that the amplitude ratio $\Gamma_0^+A_0^+/B_0^2$ is a universal constant.[33,34] Because the critical parameters for the SAFT EOS can be found only numerically (see eq 15), it is impossible to obtain the rigorous analytical expressions for the critical amplitudes B_0, A_0^+, and Γ_0^+ and to check the universality of this amplitude ratio analytically. Similar to the crossover PT EOS,[44] for the crossover SAFT EOS we can do this only numerically.

Far away from the critical point $q \gg 1$ (or $|\tau| \gg Gi$ at $v = v_c$), the crossover function $Y(q) \to 1$, the renormalized temperature and volume tend to their classical values $\bar{\tau} \to \Delta T$ and $\Delta\bar{\eta} \to \Delta v$, and eq 25 is transformed into the classical Helmholtz free energy density for the original SAFT equation of state (16). In the limit of zero density $v \to \infty$, $q \gg Gi$ for all values of the temperature and the Ginzburg number, and eq 25 is transformed into the ideal gas expression

$$\bar{A}(T, v) = -\ln(v/v_{0c}) + A_0(T) \quad (29)$$

Table 1. Constants in Equation 31 for *n*-Alkanes

coefficients $k_i^{(0)}$	coefficients $k_i^{(1)}$
$g^{(0)}$ 27.003	$g^{(1)}$ -2.3206×10^{-2}
$d_1^{(0)}$ 2.8297	$d_1^{(1)}$ -2.5844×10^{-3}
$v_1^{(0)}$ 2.6807×10^{-2}	$v_1^{(1)}$ 6.0456×10^{-5}

and equation eq 27 reproduces the ideal gas equation of state:

$$Pv = RT \quad (30)$$

4. Comparison with Experimental Data

The crossover SAFT equation of state contains the following system-dependent parameters in addition to the parameters in the original SAFT EOS: critical shifts ΔT_c and Δv_c, the Ginzburg number Gi, the rectilinear diameter amplitude d_1, the parameter v_1 in the asymmetric correction for the order parameter, and the critical amplitudes a_{20} and a_{21} in the kernel term. Because the critical parameters T_c and V_c of a pure fluid are usually known, the critical shifts can be easily determined from any classical critical parameters T_{0c} and v_{0c} obtained from a solution of equations in (15) for the SAFT EOS.

The parameters Gi, d_1, and v_1 can be found from the fit of equations 25−27 to experimental $P\rho T$ data, as are the parameters m, v^{00}, u^0, ϵ^{AB}, and κ^{AB} in the SAFT EOS. The number of segments m was considered as an additional adjustable parameter of the model in the original SAFT EOS.[10] In the present work, the parameter m for n-alkanes is taken to be an integer number equal to the number of the carbon atoms in the molecule. Because self-associated fluids are not considered in this work, we also set the association constants ϵ^{AB} and κ^{AB} equal to zero.

Critical amplitudes a_{20} and a_{21} determine the nonanalytic singular behavior of the isochoric specific heat in the critical region, and when only VLE and volumetric properties are considered, these amplitudes can be set equal to zero.[42] In a more general approach, the parameters a_{20} and a_{21} can be found from an analysis of experimental C_v or sound velocity data in the near-critical region.[42] In the present work we set $a_{20} = a_{21} = 0$, while the inverse Ginzburg number $g = 1/Gi$, the rectilinear diameter amplitude d_1, and the coefficient v_1, designed as k_i, were represented as linear functions of the molecular weight M_w,

$$k_i = k_i^{(0)} + k_i^{(1)}M_w \quad (31)$$

where parameters $k_i^{(0)}$ and $k_i^{(1)}$ were found from the analysis of the PVT and VLE data for n-hexane and n-decane with the crossover SAFT EOS. The values of these parameters are listed in Table 1.

Finally, only two adjustable parameters in the classical SAFT EOS, v^{00}, and u^0, are left. These classical parameters for all n-alkanes have been found from a fit of our model to experimental data. The values of all system-dependent parameters for methane, ethane, n-hexane, n-decane, and n-$C_{20}H_{42}$ are presented in Table 2.

For pure methane and ethane, we have adopted the same critical parameters as used earlier by Kiselev.[37] The classical parameters v^{00} and u^0 have been determined from a fit of the crossover SAFT EOS to the experimental $P\rho T$ data obtained by Kleinrahm and coworkers[51,52] and by Trappeniers et al.[53,54] for methane,

Table 2. System-Dependent Constants for the Crossover SAFT Equation of State

n-alkane	M_w	T_c, K	ρ_c, mol/L	v^{00}, mL/mol	u^0/k, K
CH_4	16.043	190.564[a]	10.122[a]	23.674	177.942
C_2H_6	30.069	305.322[a]	6.8601[a]	15.689	180.669
C_6H_{14}	86.178	507.850[b]	2.7108[b]	10.378	177.018
$C_{10}H_{22}$	142.284	617.650[c]	1.6430[c]	9.1588	179.513
$C_{20}H_{42}$	282.556	767.300[d]	0.84034[d]	9.1984	181.652
$C_{30}H_{62}$	422.826	840.350[e]	0.58292[f]	9.6289	180.288
$C_{40}H_{82}$	563.096	882.120[e]	0.39087[f]	9.7294	179.829

[a] Kiselev, ref 37. [b] Grigoryev et al., ref 58. [c] Ely, ref 59. [d] Texas A&M University, ref 63. [e] From the Hankinson−Brobst−Thomson and Rackett correlations (see ref 57, p 58). [f] Calculated with the Joback modification of Lydesen's method (see eq 33).

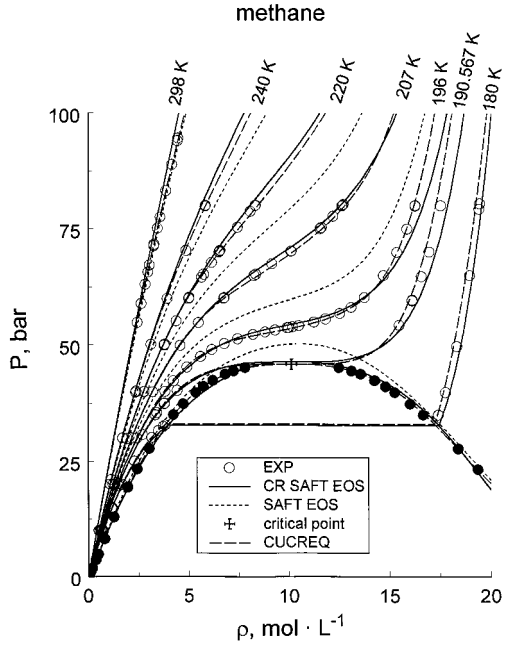

Figure 1. $P\rho T$ data[51,52] (symbols) for methane with predictions of the crossover SAFT equation of state (solid lines) and classical SAFT EOS (short-dashed lines) and with the cubic crossover EOS[44] (long-dashed lines). The open symbols correspond to the one-phase region and the filled symbols indicate VLE data.

and to selected experimental $P\rho T$ data obtained by Douslin and Harrison[55] and by Reamer et al.[56] for ethane.

Comparisons of the crossover SAFT equation of state with experimental $P\rho T$ data in the critical and supercritical regions are shown in Figures 1 and 2. As one can see, the crossover SAFT equation of state gives a good representation of the $P\rho T$ surface, especially in the critical region. The crossover SAFT EOS represents the experimental values of pressure in the critical region with an average absolute deviation (AAD) of about 0.78% ($n = 96$) in the region bounded by $0.75\rho_c \le \rho \le 1.25\rho_c$ and $T_c \le T \le 1.25T_c$, and about 2.9% in pressure for the entire set of 784 points for both substances in the region bounded by $0.05\rho_c \le p \le 2.5\rho_c$ and $T_c \le T \le 2T_c$. Comparisons of the crossover SAFT equation of state with experimental VLE data are shown in Figures 3 and 4. The figures show that the crossover SAFT EOS yields a good representation of vapor pressures and saturated liquid and vapor densities over the entire range of temperatures from the critical temperature down to the triple point. The crossover model represents the experimental saturated pressure data for both fluids with an AAD of about 3.8% ($n = 38$), the saturated liquid densities with an AAD of about 1.45% ($n = 54$), and the saturated vapor densities with an AAD of about 3.4% ($n = 18$).

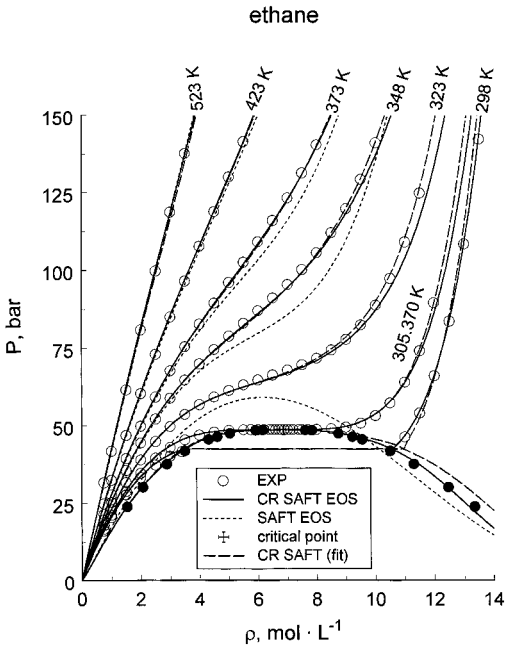

Figure 2. $P\rho T$ data[55] (symbols) for ethane with predictions of the crossover SAFT equation of state (solid lines) and classical SAFT EOS[10] (short-dashed lines) and with the five-parameter crossover SAFT model (long-dashed lines). The open symbols correspond to the one-phase region and the filled symbols indicate VLE data.

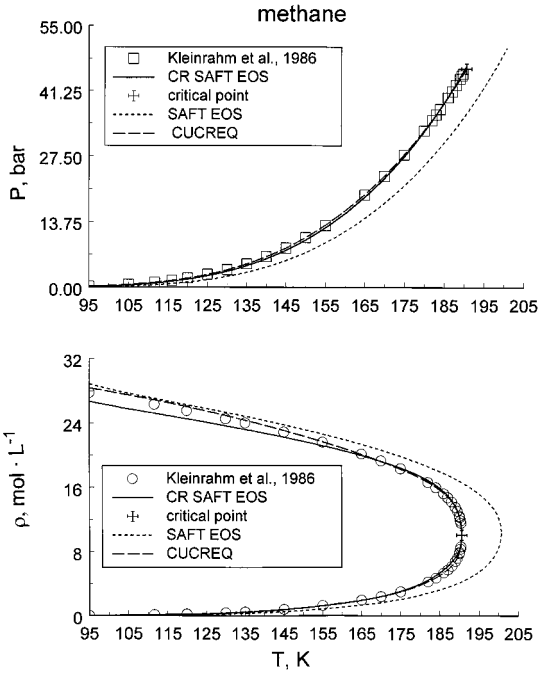

Figure 3. VLE data[51] for methane with predictions of the crossover SAFT equation of state (solid lines) and classical SAFT EOS (short-dashed lines) and with the cubic crossover EOS[44] (long-dashed lines).

For methane and ethane we can compare the crossover SAFT model not only with the original SAFT EOS obtained by Huang and Radosz,[10] but also with the cubic crossover EOS developed recently by Kiselev and Friend.[44] We need to note that for methane in the original SAFT EOS the parameter $e/k = 1$, while in this work for all substances we set $e/k = 10$. Therefore, the critical parameters shown in Figures 1 and 3 for the

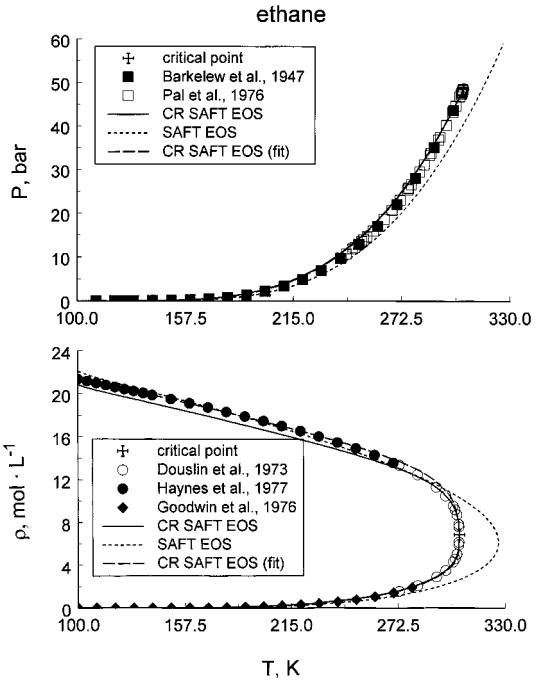

Figure 4. VLE data[55,65−63] for ethane with predictions of the crossover SAFT equation of state (solid lines) and classical SAFT EOS[10] (short-dashed lines) and with the five-parameter crossover SAFT model (long-dashed lines).

SAFT EOS differ slightly from those obtained with the original SAFT EOS.[10] The difference is small, and as one can see, the crossover SAFT equation of state gives a much better representation of the pressures and saturated densities than the original SAFT EOS,[10] especially in the critical region where the SAFT EOS yields systematic deviations up to 15−20%. However, the average deviation of pressures and the saturated densities are approximately 2 times bigger than those for the cubic crossover EOS. In principle, the representation of pressures and the saturated densities for methane and ethane with the crossover SAFT EOS can be improved if we do not use eq 31 for the parameters $g = 1/Gi$, d_1, and v_1, but find them from a fit to the experimental data (see long-dashed curve in Figures 2 and 4 for ethane). However, even in this case, a representation of the saturated pressures with the five-parameter crossover SAFT EOS for ethane and methane is worse than that achieved with the cubic crossover EOS.[44] This is mostly because of the fact that in simple fluids at low temperatures ($Gi \ll |\tau|$) the saturated liquid density is rather a cubic parabola ($\rho_L \propto |\tau|^{1/3}$; see Reid et al.[57]) than a linear function of the dimensionless temperature τ as it follows from the SAFT EOS.

For *n*-hexane and *n*-decane all parameters v^{00}, u^0, Gi, d_1, and v_1 in the crossover SAFT EOS were found from a fit to the experimental data. For the critical parameters T_c and ρ_c we adopted the values obtained by Grigoryev et al.[58] for *n*-hexane and by Ely[59] for *n*-decane. Comparisons of the crossover SAFT equation of state with *PVT* experimental data in the one-phase region for *n*-hexane and *n*-decane are shown in Figures 5 and 6 and with the VLE data in Figures 7 and 8. As one can see, with the five adjustable parameters for *n*-hexane and *n*-decane, approximately the same accuracy for the pressures and saturated densities was achieved as that for ethane and methane with only two adjustable parameters, v^{00} and u^0. However, even with five adjustable parameters, the crossover SAFT EOS gives a

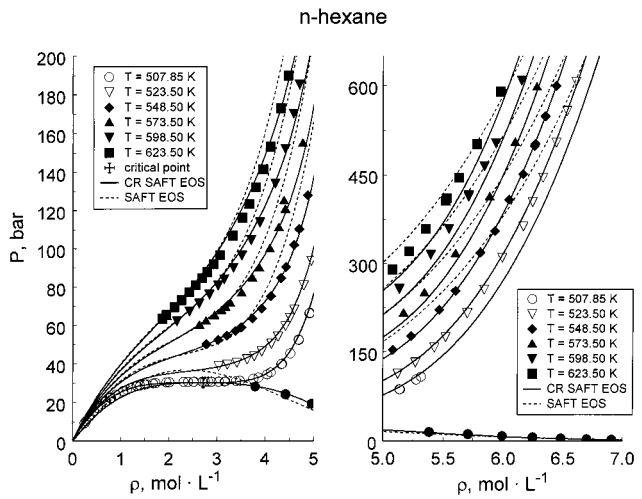

Figure 5. $P\rho T$ data[69,70] (symbols) for *n*-hexane with predictions of the crossover SAFT equation of state (solid lines) and classical SAFT EOS[10] (short-dashed lines).

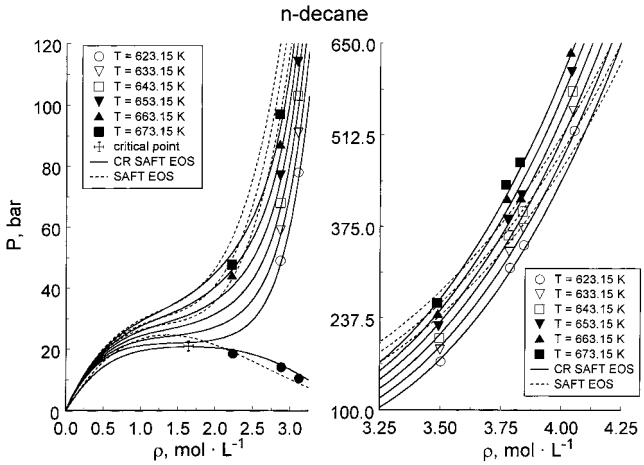

Figure 6. $P\rho T$ data[71] (symbols) for *n*-decane with predictions of the crossover SAFT equation of state (solid lines) and classical SAFT EOS (short-dashed lines).

systematic deviation up to 8−10% for the saturated liquid densities at low temperatures, $T < 0.5T_c$. These deviations are smaller than those for the original SAFT EOS (up to 12−18%) but still bigger than those for the crossover cubic model (about 1−2%).

Comparisons of the crossover SAFT equation of state with isobaric specific heat experimental data in the critical region for methane and ethane are shown in Figures 9 and 10. The crossover SAFT EOS yields not only a qualitative but also a reasonably good quantitative representation of the C_P data in the critical region, while the original SAFT EOS due to its large errors in critical point prediction does not even qualitatively describe the singular behavior; note that the curves calculated with the original SAFT EOS for ethane do not even overlap the scale for the near critical isobars shown in Figure 10.

As we mentioned above, in the present crossover EOS, the parameters a_{20} and a_{21} in eq 24 for the kernel term were set to zero. Therefore, it is not surprising that, without the kernel term, the crossover SAFT EOS cannot describe the experimental isochoric specific heat data in the asymptotic critical region within experimental uncertainty. For this purpose, the kernel term should be included and a better analytical equation of state has to be chosen as the basis of the model. However, in the

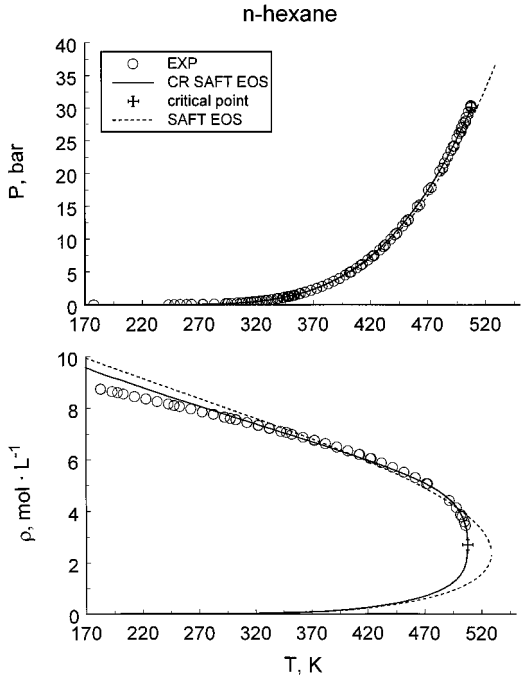

Figure 7. VLE data for *n*-hexane[70,72−80] (symbols) with predictions of the crossover SAFT equation of state (solid lines) and classical SAFT EOS[10] (short-dashed lines).

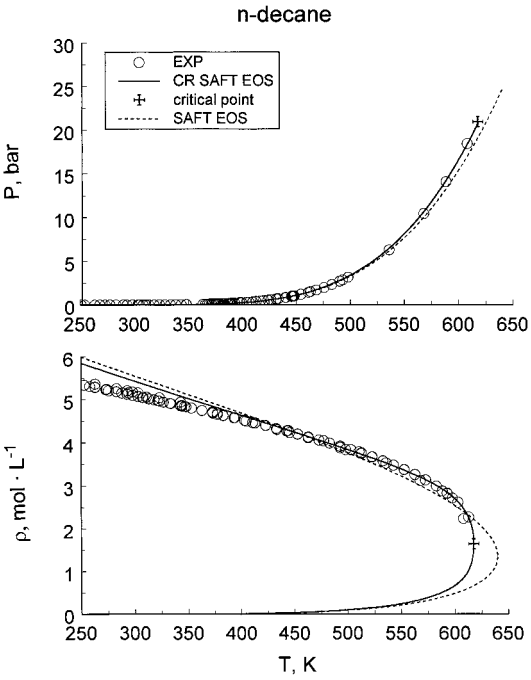

Figure 8. VLE data for *n*-decane[71,81−92] (symbols) with predictions of the crossover SAFT equation of state (solid lines) and classical SAFT EOS.[10]

present form the crossover SAFT EOS yields a satisfactory representation of the experimental C_P data in and beyond the critical region.

We are not aware of any experimental C_P data for *n*-hexane and *n*-decane in the critical and supercritical region. Therefore, in Figures 11 and 12 we show a comparison with experimental C_P data for saturated liquids obtained by Grigoryev et al.[60] and Amirkhanov et al.[61] for *n*-hexane, and by Finke et al.[62] for *n*-decane. Again, a reasonable agreement between the experimental data and values calculated with the crossover SAFT EOS is observed.

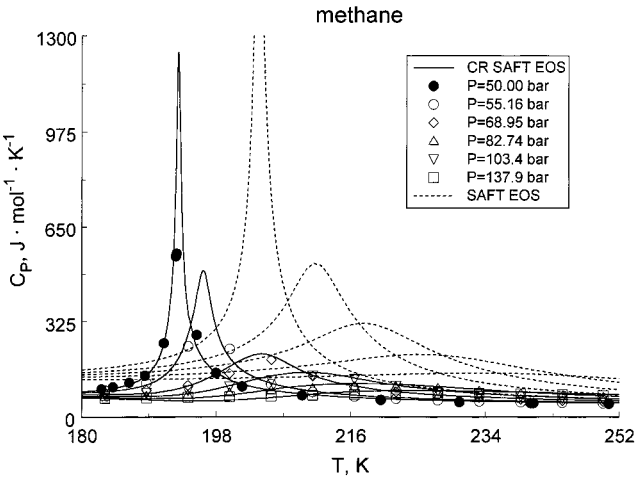

Figure 9. The isobaric specific heat data of Jones et al.[93] (empty symbols) and of van Kasteren and Zeldenrust[94] (filled symbols) for methane with predictions of the crossover SAFT equation of state (solid lines) and classical SAFT EOS[10] (short-dashed lines).

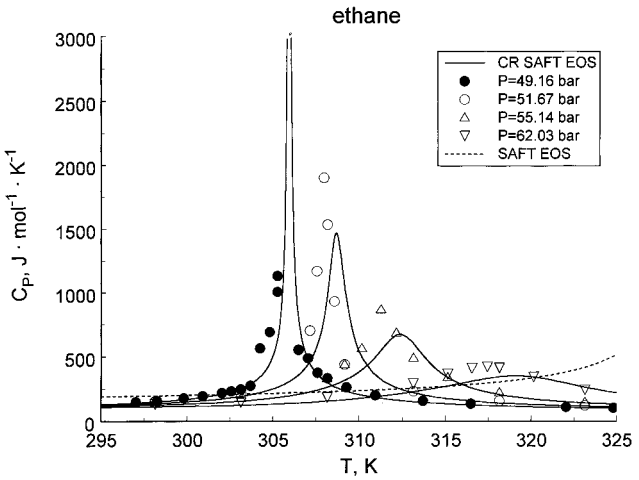

Figure 10. The isobaric specific heat data of Furtado[95] (empty symbols) and of Miazaki et al.[96] (filled symbols) for ethane with predictions of the crossover SAFT equation of state (solid lines) and classical SAFT EOS[10] (short-dashed lines).

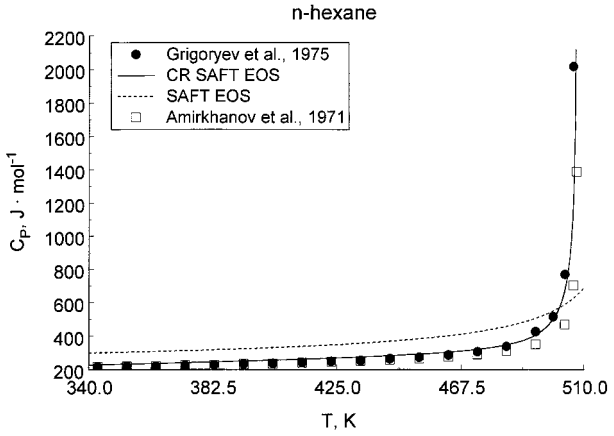

Figure 11. The saturated liquid C_P data[60,61] for *n*-hexane with predictions of the crossover SAFT equation of state (solid lines) and classical SAFT EOS[10] (short-dashed lines).

The original SAFT equation of sate was initially developed for modeling of the thermodynamic properties and the phase equilibrium of macromolecular chain fluids. Therefore, it is interesting to compare the crossover SAFT EOS with the experimental data for

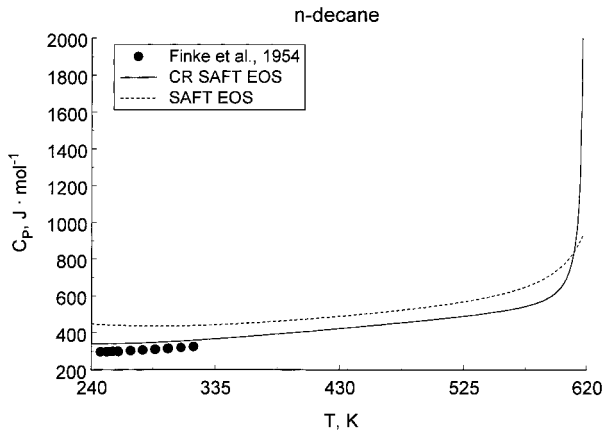

Figure 12. The saturated liquid C_P data[62] for *n*-decane with predictions of the crossover SAFT equation of state (solid lines) and classical SAFT EOS[10] (short-dashed lines).

n-alkanes with higher molecular weights, $m > 10$. In this work we applied the crossover SAFT EOS for representing the thermodynamic surface of *n*-eicosane ($C_{20}H_{42}$), *n*-triacontane ($C_{30}H_{62}$), and *n*-tetracontane ($C_{40}H_{82}$).

For the *n*-eicosane we adopted the experimental values of the critical parameters obtained in the Thermodynamics Research Center of Texas A&M University.[63] We are not aware of any experimental values of the critical parameters for *n*-alkanes with $m > 20$. Therefore, for *n*-triacontane and *n*-tetracontane we adopted the same critical temperatures as employed earlier in the Hankinson−Brobst−Thomson and the Rackett liquid−volume correlations,[57] while the critical pressure and volume we calculated with the Joback modification of Lydersen's method (see Reid et al.[57])

$$P_c = (0.113 + 0.0032m_A - 0.965\sum\Delta_P)^{-2} \quad (32)$$

$$v_c = 0.0175 + \sum\Delta_v \quad (33)$$

where for the *n*-alkanes $m_A = 3m + 2$, $\sum\Delta_P = -0.0024$, and $\sum\Delta_v = 0.13 + 0.056(m - 2)$. The values of the parameters v^{00} and u^0 for *n*-eicosane, *n*-triacontane, and *n*-tetracontane were found from a fit of the crossover SAFT model to the experimental specific volumes data obtained by Doolittle.[64] The values of all system-dependent parameters in the crossover SAFT EOS for *n*-eicosane, *n*-triacontane, and *n*-tetracontane are listed in Table 2.

A comparison of the crossover SAFT equation of state with experimental VLE data for *n*-eicosane is shown in Figure 13. The crossover model represents the experimental saturated pressure data with an AAD of about 1.3%, the saturated liquid densities with an AAD of about 1.8%, and vapor densities with an AAD of about 3.4%. Comparisons of the crossover SAFT equation of state with the experimental liquid density data are shown in Figure 14 for *n*-eicosane and Figure 15 shows results for *n*-triacontane and *n*-tetracontane. The crossover model represents the experimental liquid density data with an AAD of about 2.3% at the pressures up to 2000 bar. The dashed curves in Figures 13 and 14 show the values of pressures and densities calculated with the original SAFT EOS.[10] As one can see, even far from the critical region the crossover SAFT EOS gives a better representation of the experimental data than the original SAFT equation of state.

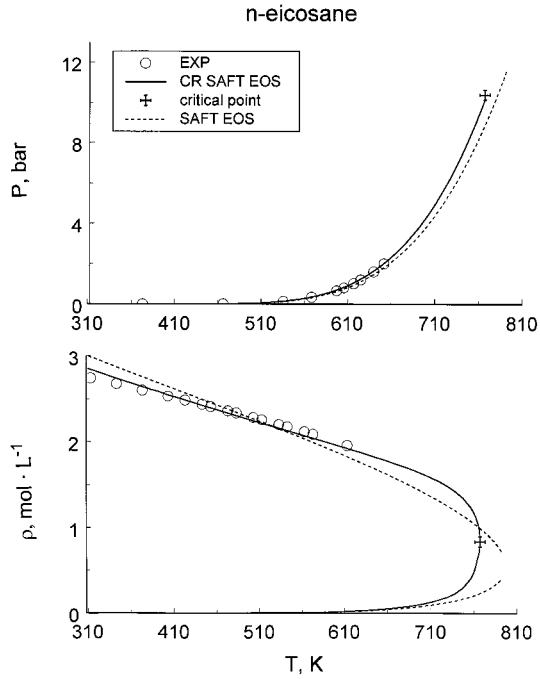

Figure 13. VLE data[64] (symbols) for *n*-eicosane with predictions of the crossover SAFT equation of state (solid lines) and classical SAFT EOS[10] (short-dashed lines).

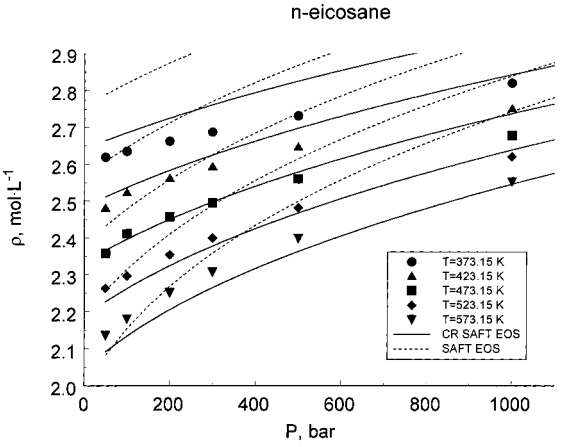

Figure 14. Liquid density data[64] (symbols) for *n*-eicosane with predictions of the crossover SAFT equation of state (solid lines) and classical SAFT EOS[10] (short-dashed lines).

For the practical application of the crossover SAFT EOS it is important to establish the relationships between the number of segments m, or molecular weight M_w, and the parameters v^{00} and u^0 of the crossover model. The parameter v^{00} has a physical meaning of the temperature-independent segment volume and the parameter u^0/k is the temperature-independent dispersion energy of interaction between segments. Because the macromolecules in the SAFT EOS are treated as the chains of the m similar segments, we expect that, in a physically consistent model, as m becomes larger, the parameters v^{00} and u^0 should not depend on the number of segments. In Figure 16 we show the parameter v^{00} as a function of the molecular weight of the *n*-alkanes. The parameter u^0 as a function of the molecular weight is shown in Figure 17. As one can see from Figure 16, for the small molecules with $M_w < 142$ ($m < 10$) the parameter v^{00} qualitatively reproduces the behavior of the critical density and decreases upon increasing the molecular weight. However, at $M_w > 142$ ($m > 10$) the

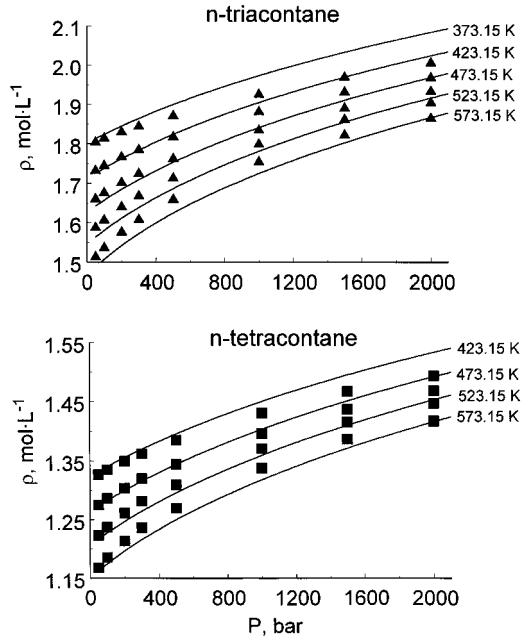

Figure 15. Liquid density data[64] (symbols) for *n*-tricontane (top) and *n*-tetracontane (bottom) with predictions of the crossover SAFT equation of state (lines).

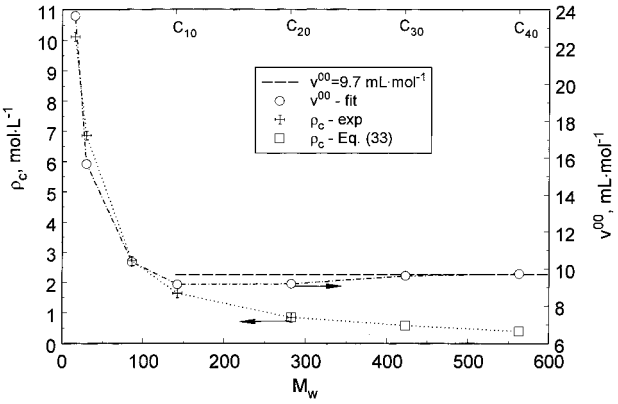

Figure 16. The critical density data (left axis) and the parameter v^{00} (right axis) for *n*-alkanes as a function of the molecular weight.

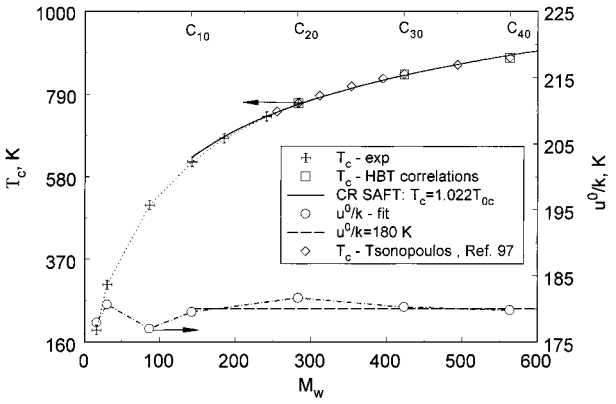

Figure 17. The critical temperature data (left axis) and the parameter u^0 (right axis) for *n*-alkanes as a function of the molecular weight.

parameter v^{00} is practically slightly increased and tends to its constant value $v^{00} \approx 9.7$ mL mol^{-1} at $M_w \geq 422$ ($m \geq 30$). Qualitatively, the same behavior is observed for the parameter u^0 (see Figure 17). For the long molecules with $M_w \geq 142$ ($m \geq 10$) the real critical temperature $T_c \approx 1.022T_{0c}$, while the parameter u^0

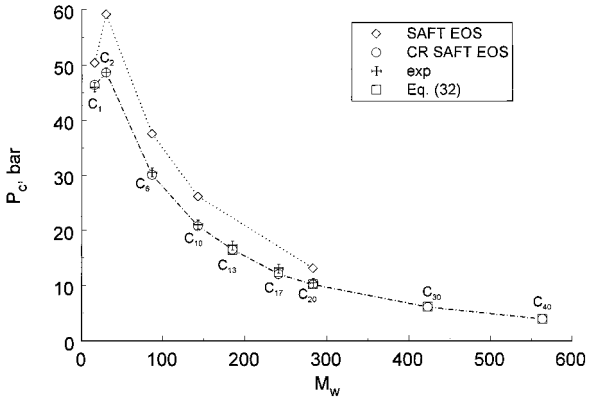

Figure 18. The critical pressure data (crosses) for *n*-alkanes with values predicted with the classical SAFT EOS[10] crossover SAFT EOS (circles) and with the Joback−Lyndersen equation (32) (squares).

exhibits small oscillations around its constant value $u^0 \approx 180$ K which is achieved at $M_w \geq 422$ ($m \geq 30$).

Thus, in the crossover SAFT EOS for the *n*-alkanes with $M_w > 142$ ($m > 10$), we can set

$$v^{00} = 9.7 \text{ mL mol}^{-1}, \quad u^0/k = 180 \text{ K}, \quad T_c = 1.022T_{0c} \text{ K} \quad (34)$$

and the critical molar volume v_c can be calculated with the Joback−Lyndersen method (see eq 33). For the *n*-alkanes with $M_w \leq 943$ ($m \leq 70$) for the crossover parameters g, d_1, and v_1, one can use eq 31 with the coefficients as given in Table 1. We do not expect that these simple linear expressions for the parameters g, d_1, and v_1 with the same coefficients will be valid at $M_w > 943$ ($m > 70$); therefore, we do not recommend applying them in this region.

A comparison of the experimental values of critical pressure with the values predicted with the crossover SAFT EOS as well as with the critical pressures calculated for the *n*-alkanes with $M_w \geq 184$ ($m \geq 13$) with the Joback−Lyndersen equation 32 is shown in Figure 18. Good agreement between experimental critical pressures and predicted values is observed. In Figure 19 we show a comparison of the experimental liquid density data for *n*-tridecane and *n*-heptadecane obtained by Doolittle[64] with the densities predicted with the crossover SAFT model with the fixed values of the coefficients v^{00} and u^0. Again, good agreement with experimental data is observed.

5. Discussion

In this paper we develop a crossover SAFT EOS on the basis of the crossover approach proposed by Kiselev.[42] In Kiselev's approach the crossover function used for renormalization of the EOS does not depend on the particular type of classical EOS to be renormalized and can be applied to any analytical equation of state. In the present paper, we use the SAFT EOS developed by Huang and Radosz[10] as an example. The crossover SAFT equation of state reproduces the nonanalytical, singular behavior asymptotically close to the critical point and is transformed into the original SAFT equation of state far from the critical point. In the limit of zero density, the crossover equation is transformed into the ideal gas equation of state. Application of this equation to PVT and VLE data for pure *n*-alkanes shows that the crossover SAFT equation yields a satisfactory

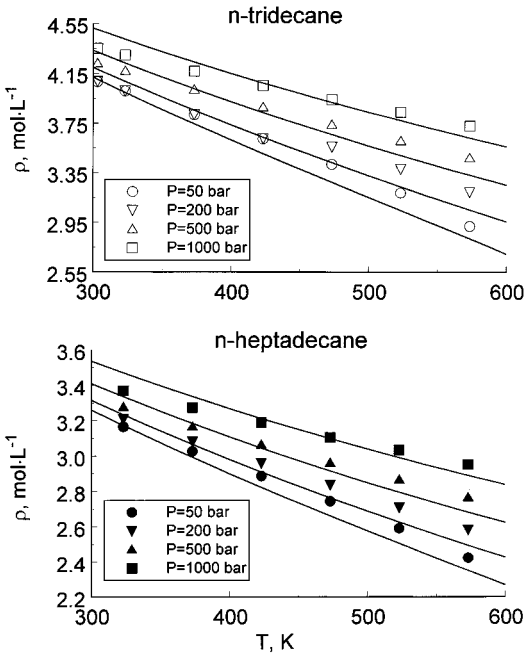

Figure 19. Liquid density data[64] (symbols) for *n*-tridecane (top) and *n*-heptadecane (bottom) with predictions of the crossover SAFT equation of state (lines).

representation of the thermodynamic surface in a temperature range from the triple point to $T \leq 2T_c$ and a density range $\rho \leq 2\rho_c$. The results of our calculations of C_P show that the crossover SAFT equation of state, unlike the classical SAFT equation of state, gives a reasonable representation of the experimental C_P data in and beyond the critical region. To improve the representation of the C_P data and extend the range of validity of our crossover equation to a wide range of densities, a better equation of state for the reference fluids must be chosen.

The method described here can also be applied to mixture calculations. Further research toward this goal is in progress and the results will be presented in the next publication.

Acknowledgment

The authors acknowledge support of the U.S. Department of Energy, Office of Basic Energy Sciences, Grant DE-FG03-95ER14568.

Nomenclature

a = Helmholtz free energy per mole (total, res, seg, chain, assoc, etc.)
a_0 = segment Helmholtz free energy per mole
a_{2i} = coefficients in the kernel term ($i = 0$ and $i = 1$)
$\bar{A}$ = dimensionless Helmholtz free energy (total, residual, etc.)
C = integration constant in eq 8
d_1 = rectilinear diameter amplitude
D_{ij} = universal constants in eq 6
Gi = Ginzburg number
g^{hs} = hard-sphere radial distribution function
K = kernel term
k = Boltzmann's constant $\approx 1.3814 \times 10^{-23}$ J/K
$k_i^{(j)}$ = coefficients in eq 31 ($j = 0$ or $j = 1$)
M = number of association sites on the molecule
M_w = molecular weight
m = number of segments
N = total number of molecules
N_A = Avogadro's number
P = pressure
P_c = critical pressure
q = measure of distance from critical point
R = gas constant
T = temperature, K
T_c = critical temperature, K
u/k = temperature-dependent dispersion energy of interaction between segments, K
u^0/k = temperature-independent dispersion energy of interaction between segments, K
V = total volume
v = molar volume
v_1 = system-dependent coefficient in eq 23
v^0 = temperature-dependent segment volume
v^{00} = temperature-independent segment volume
X^A = mole fraction of molecules NOT bonded at site A
Y = crossover function

Greek Letters

α = universal critical exponent
β = universal critical exponent
γ = universal critical exponent
Δ = difference
Δ_1 = universal critical exponent
Δv = classical order parameter
Δv_c = shift of the critical volume
$\Delta\eta$ = order parameter
$\Delta\bar{\eta}$ = rescaled order parameter
$\Delta\eta_c$ =dimensionless shift of the critical volume
ΔT = dimensionless deviation of the temperature from the classical critical temperature
$\Delta\tau_c$ = dimensionless shift of the critical temperature
δ_1 = universal constant in eq 23
τ = reduced temperature difference
$\bar{\tau}$ = rescaled reduced temperature difference
ρ = molar density
ρ_c = critical density, mol/L

Superscripts

A, B, C, ... = association sites
assoc = association
chain = chain
hs = hard sphere
ideal = ideal gas
res = residual
seg = segment

Subscripts

c = critical
0 = classical
G = gas
L = liquid

Appendix. Crossover Helmholtz Free Energy

The crossover expression for the Helmholtz free energy for the SAFT equation of state is (see eqs 25 and 26)

$$\bar{A}(T, v) = \Delta\bar{A}(\bar{\tau}, \Delta\bar{\eta}) - \Delta v\bar{P}_0(T) + \bar{A}_0^r(T) + \bar{A}_0(T) - K(\tau^2) \quad \text{(A.1)}$$

where the critical part

$$\Delta\bar{A}(\bar{\tau}, \Delta\bar{\eta}) = \bar{A}^r(\bar{\tau}, \Delta\bar{\eta}) - \bar{A}^r(\bar{\tau}, 0) - \ln(\Delta\bar{\eta} + 1) + \Delta\bar{\eta}\bar{P}_0(\bar{\tau}) \quad \text{(A.2)}$$

The dimensionless residual part of the Helmholtz free energy is given by

$$\bar{A}^{r}(\bar{\tau}, \Delta\bar{\eta}) = m\left[\frac{4\bar{\eta} - 3\bar{\eta}^2}{(1-\bar{\eta})^2} + \sum_i\sum_j D_{ij}\left(\frac{u}{kT_{0c}(\bar{\tau}+1)}\right)^i\left(\frac{\bar{\eta}}{\eta_0}\right)^j\right] + (1-m)\ln g^{hs}(\bar{\eta}) + \sum_A\left(\ln X^A - \frac{X^A}{2}\right) + \frac{1}{2}M \quad (A.3)$$

where the hard sphere distribution function g^{hs} is given by the eq 11 with account of the replacement of the reduced density η on the renormmalized value $\bar{\eta} = \eta_{0c}/(\Delta\bar{\eta}+1)$, $\eta_{0c} = \eta_0 m v^0/v_{0c}$ is the reduced critical density, and parameters v^0, u, and Δ^{AB} are given by eqs 8, 9, and 14 where temperature T is expressed through the renormalized temperature $\bar{\tau}$

$$v^0 = v^{00}\left[1 - C\exp\left(\frac{-3u^0}{kT_{0c}(\bar{\tau}+1)}\right)\right]^3 \quad (A.4)$$

$$u = u^0\left(1 + \frac{e}{kT_{0c}(\bar{\tau}+1)}\right) \quad (A.5)$$

$$\Delta^{AB} = \kappa^{AB}\frac{6\eta_0 v^{00}}{\pi N_A}[\exp(\epsilon^{AB}/kT_{0c}(\bar{\tau}+1)) - 1]g^{hs}(\bar{\eta}) \quad (A.6)$$

In eqs A.3−A.6, the parameters T_{0c} and v_{0c}, are the classical critical parameters for the original SAFT EOS determined from the solution of eq 15.

The dimensionless residual part of the Helmholtz free energy at the critical isochore $v = v_c$

$$\bar{A}^{r}(\bar{\tau}, 0) = m\left[\frac{4\bar{\eta}_{0c} - 3\bar{\eta}_{0c}^2}{(1-\bar{\eta}_{0c})^2} + \sum_i\sum_j D_{ij}\left(\frac{u}{kT_{0c}(\bar{\tau}+1)}\right)^i\left(\frac{\eta_{0c}}{\eta_0}\right)^j\right] + (1-m)\ln g^{hs}(\eta_{0c}) + \sum_A\left(\ln X^A - \frac{X^A}{2}\right) + \frac{1}{2}M \quad (A.7)$$

and

$$\bar{P}_0(\bar{\tau}) = m\left[\frac{4\eta_{0c} - 2\eta_{0c}^2}{(1-\eta_{0c})^3} + \sum_i\sum_j jD_{ij}\left(\frac{u}{kT_{0c}(\bar{\tau}+1)}\right)^i\left(\frac{\eta_{0c}}{\eta_0}\right)^j\right] + (1-m)\frac{5\eta_{0c} - 2\eta_{0c}^2}{(1-\eta_{0c})(2-\eta_{0c})} - \sum_A\left(\frac{1}{X^A} - \frac{1}{2}\right)\left(\frac{\partial X^A}{\partial\Delta\bar{\eta}}\right)_{\bar{\tau}(\Delta\bar{\eta}=0)} \quad (A.8)$$

where the renormalized temperature $\bar{\tau}$ and order parameter $\Delta\bar{\tau}$ connected to the real dimensionless temperature τ and the real order parameter $\Delta\eta$ through eqs 20 and 21.

The temperature dependent functions $\bar{A}_0^r(T)$ and $\bar{P}_0(T)$ in eq A.1 are given by

$$\bar{A}_0^{r}(T) = m\left[\frac{4\eta_{0c} - 3\eta_{0c}^2}{(1-\eta_{0c})^2} + \sum_i\sum_j D_{ij}\left(\frac{u}{kT}\right)^i\left(\frac{\eta_{0c}}{\eta_0}\right)^j\right] + (1-m)\ln g^{hs}(\eta_{0c}) + \sum_A\left(\ln X^A - \frac{X^A}{2}\right) + \frac{1}{2}M \quad (A.9)$$

and

$$\bar{P}_0(T) = m\left[\frac{4\eta_{0c} - 2\eta_{0c}^2}{(1-\eta_{0c})^3} + \sum_i\sum_j jD_{ij}\left(\frac{u}{kT}\right)^i\left(\frac{\eta_{0c}}{\eta_0}\right)^j\right] + (1-m)\frac{5\eta_{0c} - 2\eta_{0c}^2}{(1-\eta_{0c})(2-\eta_{0c})} - \sum_A\left(\frac{1}{X^A} - \frac{1}{2}\right)\left(\frac{\partial X^A}{\partial\Delta v}\right)_{T(\Delta v=0)} \quad (A.10)$$

where the hard sphere distribution function g^{hs} is given by the eq 11 with $\eta = \eta_{0c}$, and parameters v^0, u, and Δ^{AB} are given by eqs 8, 9, and 14.

Literature Cited

(1) Song, Y. H.; Lambert, S. M.; Prausnitz, J. M. *Ind. Eng. Chem. Res.* **1994**, *33*, 1047.
(2) Song, Y. H.; Lambert, S. M.; Prausnitz, J. M. *Chem. Eng. Sci.* **1994**, *49*, 2765.
(3) Lambert, S. M.; Song, Y. H.; Prausnitz, J. M. *Macromolecules* **1995**, *28*, 4866.
(4) Song, Y. H.; Hino, T.; Lambert, S. M.; Prausnitz, J. M. *Fluid Phase Equilibr.* **1996**, *117*, 69.
(5) Hino, T.; Song, Y. H.; Prausnitz, J. M. *J. Polym. Sci., Part B: Polym. Phys.* **1996**, *34*, 1977.
(6) Hino, T.; Song, Y. H.; Prausnitz, J. M. *J. Polym. Sci., Part B: Polym. Phys.* **1996**, *34*, 1961.
(7) Hino, T.; Prausnitz, J. M. *Fluid Phase Equilibr.* **1997**, *138*, 105.
(8) Hino, T.; Prausnitz, J. M. *Macromolecules* **1998**, *31*, 2636.
(9) Chapman, W. G.; Gubbins, K. E.; Jackson, G.; Radosz, M. *Ind. Eng. Chem. Res.* **1990**, *29*, 1709.
(10) Huang, H. S.; Radosz, M. *Ind. Eng. Chem. Res.* **1990**, *29*, 2284.
(11) Banaszak, M.; Chiew, Y. C.; Radosz, M. *Phys. Rev. E* **1993**, *48*, 3760.
(12) Banaszak, M.; Chiew, Y. C.; O'Lenick, R.; Radosz, M. *J. Chem. Phys.* **1994**, *100*, 3803.
(13) Ghonasgi, D.; Chapman, W. G. *J. Chem. Phys.* **1994**, *100*, 6633.
(14) Gil-Villegas, A.; Galindo, A.; Whitehead, P. J.; Mills, S. J.; Jackson, G.; Burgess, A. N. *J. Chem. Phys.* **1996**, *106*, 4168.
(15) Galindo, A.; Davies, L. A.; Gil-Villegas, A.; Jackson, G. *Mol. Phys.* **1998**, *93*, 241.
(16) Blas, F. J.; Vega, L. F. *Ind. Eng. Chem. Res.* **1998**, *37*, 660.
(17) Adidharma, H.; Radosz, M. *Fluid Phase Equilibr.* **1999**, *158−160*, 165.
(18) Adidharma, H.; Radosz, M. *Fluid Phase Equilibr.* **1999**, *161*, 1.
(19) Redlich, O.; Kwong, J. N. S. *Chem. Rev.* **1949**, *44*, 233.
(20) Soave, G. *Chem. Eng. Sci.* **1972**, *27*, 1197.
(21) Peng, D. Y.; Robinson, D. B. *Chem. Eng. Sci.* **1976**, *15*, 59.
(22) Peters, C. J.; Arons, J. D.; Levelt Sengers, J. M. H.; Gallagher, J. S. *AIChE J.* **1988**, *34*, 834.
(23) Magoulas, K.; Tassios, D. *Fluid Phase Equilibr.* **1990**, *56*, 119.
(24) Voros, N.; Stamataki, S.; Tassios, D. *Fluid Phase Equilibr.* **1994**, *96*, 51.

(25) Solimando, R.; Rogalsky, M.; Neau, E.; Peneloux, A. *Fluid Phase Equilibr.* **1995**, *106*, 59.
(26) Peng, C.-L.; Stein, F. P.; Gow, A. S. *Fluid Phase Equilibr.* **1995**, *108*, 79.
(27) Zielke, F.; Lempe, D. A. *Fluid Phase Equilibr.* **1997**, *141*, 63.
(28) Fermeglia, M.; Bertucco, A.; Patrizio, D. *Chem. Eng. Sci.* **1997**, *52*, 1517.
(29) Fermeglia, M.; Bertucco, A.; Bruni, S. *Chem. Eng. Sci.* **1998**, *53*, 1517.
(30) Gregg, C. J.; Stein, F. P.; Radosz, M. *Ind. Eng. Chem. Res.* **1990**, *29*, 1709.
(31) Wu, C. S.; Chen, Y. P. *Fluid Phase Equilibr.* **1994**, *100*, 103.
(32) McCabe, C.; Galindo, A.; Gil-Villegas, A.; Jackson, J. *Int. J. Thermophys.* **1998**, *19*, 1511.
(33) Sengers, J. V.; Levelt Sengers, J. M. H. *Annu. Rev. Phys. Chem.* **1986**, *37*, 189.
(34) Anisimov, M. A.; Kiselev, S. B. Universal Crossover Approach to Description of Thermodynamic Properties Fluids and Fluid Mixtures; In *Thermal Physics Reviews*; Sheindlin, A. E., Fortov, V. E., Eds.; Harwood Academic Publishers GmbH: New York, 1992; Vol. 3, Part 2.
(35) Jin, G. X.; Tang, S.; Sengers, J. V. *Phys. Rev. E* **1993**, *47*, 388.
(36) Povodyrev, A. A.; Jin, G. X.; Kiselev, S. B.; Sengers, J. V. *Int. J. Thermophys.* **1996**, *17*, 909.
(37) Kiselev, S. B. *Fluid Phase Equilibr.* **1997**, *128*, 1.
(38) Kiselev, S. B.; Rainwater, J. C. *Fluid Phase Equilibr.* **1997**, *141*, 129.
(39) Kiselev, S. B.; Rainwater, J. C.; Huber, M. L. *Fluid Phase Equilibr.* **1998**, *150*−*151*, 469.
(40) Kiselev, S. B.; Huber, M. L. *Int. J. Refrig.* **1998**, *21*, 64.
(41) Kiselev, S. B.; Rainwater, J. C. *J. Chem. Phys.* **1998**, *109*, 643.
(42) Kiselev, S. B. *Fluid Phase Equilibr.* **1998**, *147*, 7.
(43) Patel, N. C.; Teja, A. S. *Chem. Eng. Sci.* **1982**, *37*, 463.
(44) Kiselev, S. B.; Friend, D. G. *Fluid Phase Equilibr.* **1999**, *162*, 51.
(45) Kostrowicka Wyczalkowska, A.; Anisimov, M. A.; Sengers, J. V. *Fluid Phase Equilibr.* **1999**, *158*−*160*, 523.
(46) Carnahan, N. F.; Starling, K. E. *J. Chem. Phys.* **1969**, *51*, 635.
(47) Alder, B. J.; Young, D. A.; Mark, M. A. *J. Chem. Phys.* **1972**, *56*, 3013.
(48) Chen, S. S.; Kreglewski, A. *Ber. Bunsen-Ges. Phys. Chem.* **1977**, *81*, 1048.
(49) Belyakov, M. Y.; Kiselev, S. B.; Rainwater, J. C. *J. Chem. Phys.* **1997**, *107*, 3085.
(50) Kiselev, S. B.; Friend, D. G. *Fluid Phase Equilibr.* **1999**, *155*, 33.
(51) Kleinrahm, R.; Duschek, W.; Wagner, W. *J. Chem. Thermodyn.* **1986**, *18*, 1103.
(52) Handel, G.; Kleinrahm, R.; Wagner, W. *J. Chem. Thermodyn.* **1992**, *24*, 685.
(53) Trappeniers, N. G.; Wassenaar, T.; Abels, J. C. *Physica A* **1979**, *98*, 289.
(54) Trappeniers, N. G.; Wassenaar, T.; Abels, J. C. *Physica A* **1980**, *100*, 660.
(55) Douslin, D. R.; Harrison, R. H. *J. Chem. Thermodyn.* **1973**, *5*, 491.
(56) Reamer, H. H.; Olds, R. H.; Sage, B. H.; Lacey, W. N. *Ind. Eng. Chem.* **1944**, *36*, 957.
(57) Reid, C. R.; Prausnitz, J. M.; Polling, B. E. *The Properties of Gases and Liquids*, 4th ed.; McGraw-Hill, Inc.: New York, 1987.
(58) Grigoryev, B. A.; Rastorguyev, Y. L.; Gerasimov, A. A.; Kurumov, D. S.; Plotnikov, S. A. *Int. J. Thermophys.* **1988**, *9*, 439.
(59) Ely, J. F. Colorado School of Mines, unpublished results.
(60) Grigoryev, B. A.; Rastorguev, Y. L.; Yanin, G. S. *Izv. Vyssh. Ucheb. Zaved.* (Ser.: Neft and Gaz (Russian)) **1975**, *10*, 63.
(61) Amirkhanov, Kh. I.; Alibekov, B. G.; Vikhrov, D. I.; Mirskaya, V. A.; Levina, L. N. *High Temp.* **1971**, *9*, 1211.
(62) Finke, H. L.; Gross, M. E.; Waddington, G.; Huffman, H. M. *J. Am. Chem. Soc.* **1954**, *41*, 333.
(63) Texas A&M University. *Selected Values of Properties of Hydrocarbons and Related Compounds*; Thermodynamics Research Center: College Station, TX, 1984.
(64) Doolittle, A. K. *J. Chem. Eng. Data* **1964**, *9*, 275.
(65) Barkelew, C. H.; Valentine, J. L.; Hurd, C. O. *Trans. Am. Inst. Chem. Eng.* **1947**, *43*, 25.
(66) Goodwin, R. D.; Roder, H. M.; Straty, G. S. Technical Note 684; National Bureau of Standards (U.S.): Gaithersburg, MD, 1976.
(67) Pal, A. K.; Pope, G. A.; Arai, Y.; Carnahan, N. F.; Kobayashi, R. *J. Chem. Eng. Data* **1976**, *21*, 394.
(68) Haynes, W. M.; Hiza, M. J. *J. Chem. Thermodyn.* **1977**, *9*, 179.
(69) Kurumov, D. S.; Grigoryev, B. A. *Izv. Vyssh. Ucheb. Zaved.* (Ser.: Neft and Gaz (Russian)) **1983**, *26*, 36.
(70) Kurumov, D. S.; Grigoryev, B. A. *Rus. J. Phys. Chem.* **1986**, *56*, 338.
(71) Gehrig, M.; Lentz, H. *Erdoel Kohle-Erdgas Pet.* **1983**, *36*, 277.
(72) Daridon, J. L.; Lagourette, B.; Grolier, J.-P. E. *Int. J. Thermophys.* **1998**, *19*, 145.
(73) Ellis, J. A.; Chao, K. C. *J. Chem. Eng. Data* **1973**, *18*, 264.
(74) Genco, J.; Teja, A.; Kay, W. *J.Chem. Eng. Data* **1980**, *25*, 355.
(75) Kay, W. B.; Hoffman, R.; Davies, O. *J. Chem. Eng. Data* **1975**, *20*, 333.
(76) Mousa, A. H. N. *J. Chem. Thermodyn.* **1977**, *9*, 1063.
(77) Sauermann, P.; Holzapfel, K.; DeLoos, T. W. *Fluid Phase Equilibr.* **1995**, *112*, 249.
(78) Shim, J.; Kohn, J. P. *J. Chem. Eng. Data* **1962**, *7*, 3.
(79) Thomas, G. L.; Young, S. *J. Chem. Soc.* **1895**, *67*, 1071.
(80) Wieczorek, S. A.; Stecki, J. *J. Chem. Thermodyn.* **1978**, *10*, 177.
(81) Alcart, E.; Tardajos, G.; Pena, M. D. *J. Chem. Eng. Data* **1981**, *26*, 22.
(82) Allemand, N.; Jose, J.; Merlin, J. C. *Thermochim. Acta* **1986**, *105*, 79.
(83) Beaudoin, J. M.; Kohn, J. P. *J. Chem. Eng. Data* **1967**, *12*, 189.
(84) Carruth, G. F.; Kobayashi, R. *J. Chem. Eng. Data* **1973**, *18*, 115.
(85) Chirico, R. D.; Nguyen, A.; Steele, W. V.; Strube, M. M.; Tsonopoulos, C. *J. Chem. Eng. Data* **1989**, *34*, 149.
(86) Dornte, R. W.; Smyth, C. P. *J. Am. Chem. Soc.* **1930**, *52*, 3546.
(87) Francis, A. W. *Ind. Eng. Chem.* **1957**, *49*, 1779.
(88) Gregorowicz, J.; Kiciak, K.; Malanowski, S. *Fluid Phase Equilibr.* **1987**, *38*, 97.
(89) Reamer, H. H.; Olds, R. H.; Sage, B. H.; Lacey, W. N. *Ind. Eng. Chem.* **1942**, *34*, 1526.
(90) Sage, B. H.; Lavander, H. M.; Lacey, W. N. *Ind. Eng. Chem.* **1940**, *32*, 743.
(91) Texas A&M University. *Selected Values of Properties of Hydrocarbons and Related Compounds*; Thermodynamics Research Center: College Station, TX, 1980.
(92) Willingham, C. B.; Taylor, W. J.; Pignocco, J. M.; Rossini, F. D. *J. Res. NBS* **1945**, *35*, 219.
(93) Jones, M. L.; Mage, D. T.; Faulkner, R. C.; Katz, D. L. *Chem. Eng. Prog. Symp. Ser.* **1963**, *59*, 52.
(94) van Kasteren, P. H. G.; Zeldenrust, H. *Ind. Eng. Chem. Fundam.* **1979**, *18*, 333.
(95) Furtado, A. Ph.D. Thesis, Department of Chemical Engineering, University of Michigan, Ann Arbor, MI, 1973.
(96) Miazaki, T.; Hejmadi, A. V.; Powers, J. E. *J. Chem. Thermodyn.* **1992**, *12*, 105.
(97) Tsonopoulos, C. *AIChE J.* **1987**, *33*, 2080.

Received for review June 1, 1999
Revised manuscript received September 8, 1999
Accepted September 16, 1999

IE990387I